한국기계가공학회지, 제19권, 제9호, pp. 15～23(2020.09) ISSN 1598-6721(Print)
Journal of the Korean Society of Manufacturing Process Engineers, Vol. 19, No. 9, pp. 15～23(2020.09) ISSN 2288-0771(Online)

https://doi.org/10.14775/ksmpe.2020.19.09.015

A Study on the Backward Extrusion of Internal Spline

YongIl Cho*, JongUng Choi**, Yuangen Qiu*, Heayong Cho***,#

* Department of Mechanical Engineering of Chungbuk National University, Korea,
** LS Industrial Systems, Electrotenology R&D Center, CheongJu, Korea,
*** Department of Mechanical Engineering of Chungbuk National University, Korea,

내부 스플라인의 후방압출에 관한 연구

조용일*, 최종웅, 추연근*, 조해용***,#**

*충북대학교 기계공학과, **LS전기 전력연구소, ***충북대학교 기계공학부

(Received 24 July 2020; received in revised form 20 August 2020; accepted 28 August 2020)

ABSTRACT

Spline is a machine component using transmits rotating energy with grooves on internal of boss and external periphery of shaft. Internal spline is generally produced by machining process. However, to reduce manufacturing cost and save time, plastic deformation process such as backward extrusion is gradually adapted for spline production. In plastic deformation process, forming load, stress on tools and flow flaws should be taken into account to have sound products. For this purpose, kinematically admissible velocity fields for Upper Bound Method in backward extrusion of internal spline has been suggested, then forming load and relative pressure have been calculated. Internal spline forming experiments have been con-ucted under hydraulic press and the calculated forming load well predicts the load of experiment.

Keywords : Backward Extrusion(후방압출), Cold Forging(냉간 단조), Upper Bound Solution(상계해), Internal Spline(내부 스플라인)

1. Introduction

Internal splines are widely used in the industries of automobile, aircraft and vessels etc. Two groups of manufacturing methods for internal splines; cutting ways such as broaching, shaping and non-cutting ways such as threading, extrusion are available in engineering industry. Generally, in internal spline manufacturing, spline is shaped by machining followed drilling hole in solid shaft. This machining ways cut grain flow of raw material and this caused deterioration of mechanical characteristics of strength and ductility. In addition, machining process is relatively high cost and time consuming way.

On the contrary, forming process has formed flow lines continuously along tool surface and makes strength higher and ductility better. Also, it could

Corresponding Author : hycho@cbnu.ac.kr
Tel: +82-43-261-2464, Fax: +82-43-263-2441

Copyright Ⓒ The Korean Society of Manufacturing Process Engineers. This is an Open-Access article distributed under the terms of the Creative Commons Attribution-Noncommercial 3.0 License (CC BY-NC 3.0 http://creativecommons.org/licenses/by-nc/3.0) which permits unrestricted non-commercial use, distribution, and reproduction in any medium, provided the original work is properly cited.

save raw material and improve productivity compare to machining. Hence, many studies have been published to give solutions in forming process.[1~2]

Yang et. al[3] had suggested kinematically admissible velocity field taking into account 3D effect which could be applied to ellipsoidal shaped tube backward extrusion. Lee et. al[4] had predicted backward and forward extrusion load of wrench bolt having a regular polygon shaped grooves by means of upper bound method. Wang et. al[5,6] study forward extrusion of internal spline with long tube shaped material and designed mandrel shape with FEM. The studies which have been done are mainly focus on closed die forging and forward extrusion with hollow material compare to backward extrusion with solid material.

This paper describes internal spline forming process by means of backward extrusion with solid billet and calculates forming load with upper bound method. To get upper bound solution, a kinematically admissibility velocity field for internal spline backward extrusion has been suggested. The validity of suggest velocity field has been investigated by comparison between calculated and experimented loads.

2. Velocity Fields

Upper bound method gives approximated solution with velocity fields while having an exact solution is difficult to have in forming process. With higher load value than real one in forming process, it is useful to predict process conditions and forming load

2.1 Nomenclature

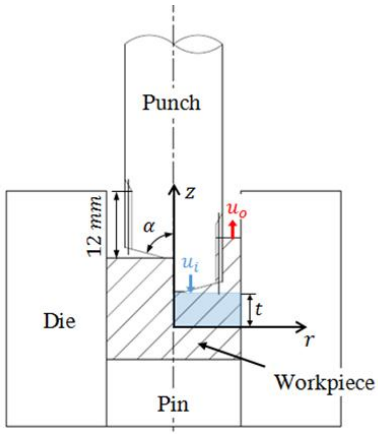

Fig. 1 Schematic drawing of backward extrusion

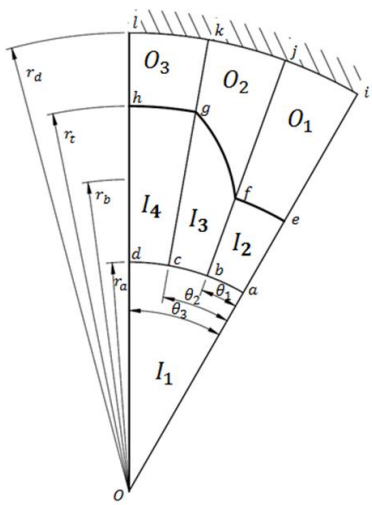

Fig. 2 Deformation regions for half pitch of internal spline

r, θ, z : cylindrical coordinate system
m : friction constant factor
P : Forming load (kN)
R : Involute curve
P_{av} : Average pressure (N/m^2)
M : Module [mm]
N : Number of teeth
r_a : Radius of Zone I_1 [mm]
r_b : base circle radius [mm]
r_d : Tool radius [mm]

r_t : tip circle radius [mm]
U_r, U_θ, U_z : Velocity component [m/s]
$|\Delta V|$: Velocity discontinuity
α : Half pitch angle [rad.]
t : Thickness of deformed area [mm]
U_o : Extrusion velocity [m/s]
$\dot{W}_f$: Friction energy dissipation rate
$\dot{W}i$: Internal energy dissipation rate
$\dot{W}s$: Shear energy dissipation rate
$\dot{W}t$: Total energy dissipation rate
$\dot{\epsilon}$: Strain rate , $\bar{\dot{\varepsilon}}$: Effective strain rate
θ_1 : Angel of in base circle area,
θ_2 : Angle in toothed area,
θ_3 : Angle in symmetric area
$\bar{\sigma}$: Mean flow stress

Geometric relationship of backward extrusion from solid billet was shown in Fig. 1 under cylindrical coordinate system of r, Θ, z. The half pitch of internal spline could be divided into 7 regions as shown in Fig. 2.

The billet is assumed as incompressible, isotropic and rigid plastic material and constant friction condition between tool and material is implemented while the deformed material obeys Von-Mises yield criteria and punch end surface keeps flat.

2.2 Kinematically admissible velocity fields

Kinematically admissible velocity field shows material flow in mathematically. With volume constancy and boundary condition at and between each deformation regions, the velocity fields could be derived as follow;

2.1.1 Region I_1 $(0 \le \theta \le \theta_3,\ 0 \le r \le r_a)$

$$U_r = \frac{u_i r z}{t^2} \tag{1}$$

$$U_\theta = 0 \tag{2}$$

$$U_z = -\frac{u_i z^2}{t^2} \tag{3}$$

2.1.2 Region I_2 $(0 \le \theta \le \theta_1,\ r_a \le r \le r_b)$

$$U_r = \frac{u_i z\left\{r^2(2r-3r_b) - r_a^2(2r_a-3r_b)\right\}}{3rt^2(r_a-r_b)} + \frac{u_i r_a^2 z}{rt^2} \tag{4}$$

$$U_\theta = 0 \tag{5}$$

$$U_z = -\frac{u_i z^2(r-r_b)}{t^2(r_a-r_b)} \tag{6}$$

2.1.3 Region I_3 $(\theta_1 \le \theta \le \theta_2,\ r_a \le r \le R)$

Where, R(Θ) represents involute curvature(FG) and expresses as follows;

$$\theta = \theta_1 + \frac{\sqrt{R(\theta)^2 - r_b^2}}{r_b} - \tan^{-1}\frac{\sqrt{R(\theta)^2 - r_b^2}}{r_b} \tag{7}$$

$$U_r = \frac{u_i z\left\{r^2(2r-3R) - r_a^2(2r_a-3R)\right\}}{3rt^2(r_a-R)} + \frac{u_i r_a^2 z}{rt^2} \tag{8}$$

$$U_\theta = 0 \tag{9}$$

$$U_z = -\frac{u_i z^2(r-R)}{t^2(r_a-R)} \tag{10}$$

2.1.4 Region I_4 $(\theta_2 \le \theta \le \theta_3,\ r_a \le r \le r_t)$

$$U_r = \frac{u_i z\left\{r^2(2r-3r_t) - r_a^2(2r_a-3r_t)\right\}}{3rt^2(r_a-r_t)} + \frac{u_i r_a^2 z}{rt^2} \tag{11}$$

$$U_\theta = 0 \tag{12}$$

$$U_z = -\frac{u_i z^2 (r - r_t)}{t^2 (r_a - r_t)} \tag{13}$$

2.1.5 Region O_1 ($0 \le \theta \le \theta_1$, $r_b \le r \le r_d$)

$$U_r = \frac{L(r - r_d)}{(r_b - r_d)} \tag{14}$$

where, $$L = \frac{u_i z (r_a^2 + r_a r_b + r_b^2)}{3t^2 r_b} \tag{15}$$

$$U_\theta = -\frac{\{Lt^2(2r - r_d) - 2u_o rz(r - r_b)\}\theta}{t^2 (r_b - r_d)} \tag{16}$$

$$U_z = \frac{u_o z^2 (r - r_b)}{t^2 (r_d - r_b)} \tag{17}$$

2.1.6 Region O_2 ($\theta_1 \le \theta \le \theta_2$, $R \le r \le r_d$)

$$U_r = \frac{M(r - r_d)}{(R - r_d)} \tag{18}$$

where, $$M = \frac{u_i z \{r_a^2 + r_a R + R^2\}}{3Rt^2} \tag{19}$$

$$U_\theta = I(\theta, z) - I(\theta_1, z) - \frac{Lt^2 \theta_1 (2r - r_d) - 2u_0 \theta_1 rz(r - r_b)}{t^2 (r_b - r_d)} \tag{20}$$

where,

$$I(\theta, z) = -\int \frac{Mt^2(2r - r_d) - 2u_o z(r^2 - rR)}{t^2 (R - r_d)} d\theta \tag{21}$$

$$U_z = \frac{u_o z^2 (r - R)}{t^2 (r_d - R)} \tag{22}$$

2.1.7 Region O_3 ($\theta_2 \le \theta \le \theta_3$, $r_t \le r \le r_d$)

$$U_r = \frac{N(r - r_d)}{(r_t - r_d)} \tag{23}$$

$$U_\theta = -\frac{\{Nt^2(2r - r_d) - 2u_o rz(r - r_t)\}(\theta - \theta_2)}{t^2 (r_t - r_d)} + U_{\theta, O_2}(r, \theta_2, z) \tag{24}$$

2.3 Internal Energy dissipation rate calculation

Strain rate under cylindrical coordinate system could be derived from velocity fields as follows;

$$\begin{aligned} U_z &= \frac{u_o z^2 (r - r_t)}{t^2 (r_d - r_t)} \\ \dot{\epsilon}_r &= \frac{\partial U_r}{\partial r} \\ \dot{\epsilon}_\theta &= \frac{1}{r}\left(\frac{\partial U_\theta}{\partial \theta} + U_r\right) \\ \dot{\epsilon}_z &= \frac{\partial U_z}{\partial z} \\ \dot{\epsilon}_{r\theta} &= \frac{1}{2}\left(\frac{\partial U_\theta}{\partial r} + \frac{1}{r}\frac{\partial U_r}{\partial \theta} - \frac{U_\theta}{r}\right) \\ \dot{\epsilon}_{\theta z} &= \frac{1}{2}\left(\frac{1}{r}\frac{\partial U_z}{\partial \theta} + \frac{\partial U_\theta}{\partial z}\right) \\ \dot{\epsilon}_{rz} &= \frac{1}{2}\left(\frac{\partial U_r}{\partial z} + \frac{\partial U_z}{\partial r}\right) \end{aligned} \tag{25, 26}$$

The effective strain rate is calculated with strain rates with Eq.

$$\dot{\bar{\epsilon}} = \frac{2}{\sqrt{3}}\{(\dot{\epsilon}_r^2 + \dot{\epsilon}_\theta^2 + \dot{\epsilon}_z^2)/2 + (\dot{\epsilon}_{r\theta}^2 + \dot{\epsilon}_{\theta z}^2 + \dot{\epsilon}_{zr}^2)\}^{1/2} \tag{27}$$

Total internal energy dissipation rate is the sum of each deformation region's internal energy dissipation rate according to Eq. (28)

$$\dot{W}_i = \int_V \bar{\sigma}\dot{\bar{\epsilon}}\, dV \tag{28}$$

where, $dV = r \cdot dr \cdot d\theta \cdot dz$.

2.4 Shear energy dissipation rate

At interfaces surfaces between deformation regions such as ef, fg, gh, eijf, flkg, gklh, shear energy dissipation rate caused by velocity inconsistency is calculated with Eq. (29)

$$\dot{W}_s = \int_S \tau |\Delta V| dS \tag{29}$$

Where, τ is pure shear yield stress of material and its value is $\bar{\sigma}/\sqrt{3}$. $|\Delta V|$ is relative velocity value on the surfaces.

2.5 Friction energy dissipation rate

On contact surfaces between material and tool such as ij, jk and between material and punch such as oad, aefb, bfgc, cghd, friction energy is occurred by velocity differences. The friction energy is calculated with Eq. (30)

$$\dot{W}_f = \int_S m\tau |\Delta V| dS \quad (0<m<1) \tag{30}$$

2.6 Total energy dissipation rate

Total energy is the sum of each energy component calculated from Eq. (28), Eq. (29) and Eq. (30).

$$\dot{W}_t = \sum \dot{W}_i + \sum \dot{W}_s + \sum \dot{W}_f \tag{31}$$

3. Results and Discussion

This paper suggests velocity fields for backward extrusion with solid billet. The material using for upper bound analysis is SCM 435 and the flow stress taking into account work hardening was calculated with Eq. (32)

$$\bar{\sigma} = 873\epsilon^{0.14} \tag{32}$$

The specification of experimented spline is 1.35 mm of tooth height, 75º of conical angle at punch tip, 0.08 of friction constant, 8 ~ 12 teeth and 0.6 ~ 0.8 of nominal diameter ratio. Table 1 shows detail specification.

Table 1 Specifications of design variables

	Nominal diameter ratio (d_n/d_d)			Number of teeth		
	0.6	0.7	0.8	8	10	12
θ_1	4.2°			11.7°	7.2	4.2°
θ_2	8.95°			16.4°	11.9°	8.9°
θ_3	15°			22.5°	18°	15°
r_b (mm)	5.325	6.325	7.325	6.45		
r_t (mm)	6.675	9.675	8.675	7.8		
r_d (mm)	10			10		

Nominal diameter ratio is ratio of nominal diameter (d_n) to tool diameter (d_d) and designated as Eq. (33)

$$\frac{d_n}{d_d} = \frac{r_b + r_t}{2r_d} \tag{33}$$

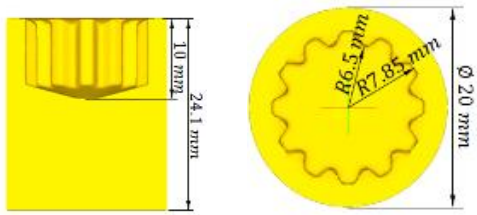

Fig. 3 Simulated results of backward extrusion for nominal diameter ratio 0.71

3.1 Finite Element Analysis results

From FEM results, it is predicted that no flow flaw like folding or under filling in forming process. Fig. 3 shows analytical results with internal spline having 0.71 of nominal diameter ratio. The punch tip angle of entrance and depth is 30º and 10 mm, respectively for backward extrusion.

Friction area between material and punch at tip circle of internal spline is bigger than that of at base circle. Therefore, because rising velocity of material at tip circle gets slower than outer area, it is considered that top end teeth surface was formed in reclined. In case of internal spline forming with backward extrusion, a deeper forming stoke is needed to have right dimension in height by this reclining at top surface.

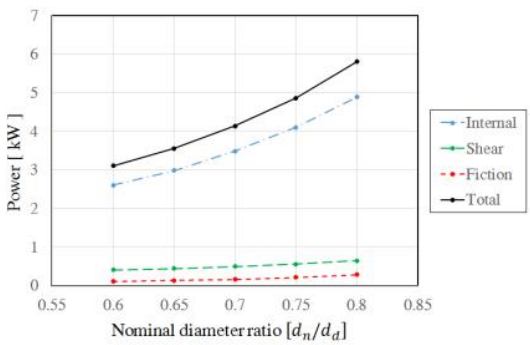

Fig. 4 Relationship between power and nominal diameter ratio at 12 teeth of internal spline

3.2 Upper bound analysis results

When nominal diameter ratio is 0.71, each energy dissipation rate portion is 84% of internal, 12% of shear while 4 % of friction. Internal energy dissipation rate is much higher than other two ones. From this result, it is known that required forming energy is mainly caused by internal deformation of material and it is considered that the induced velocity is reasonable to predict forming load of backward extrusion for internal spline. As the nominal diameter ratio increases, energy dissipation rate also increase and 0.8 of nominal diameter ratio case has almost double times higher than that of 0.6 in energy dissipation rate.

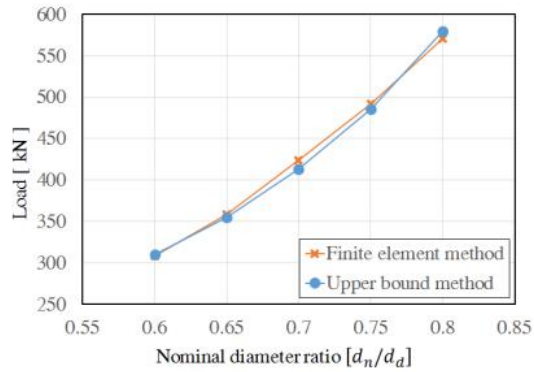

(a) load and nominal diameter ratio

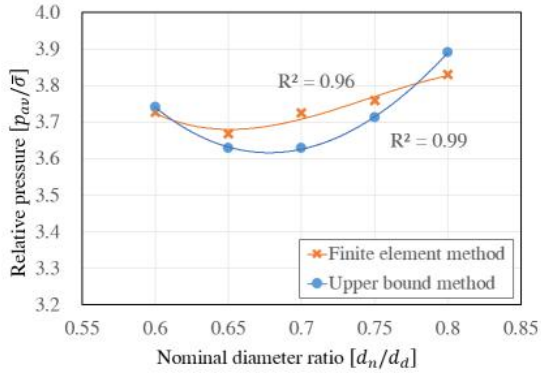

(b) relative pressure and nominal diameter ratio

Fig. 5 Comparisons of upper bound analysis and FEM at 12 teeth of internal spline

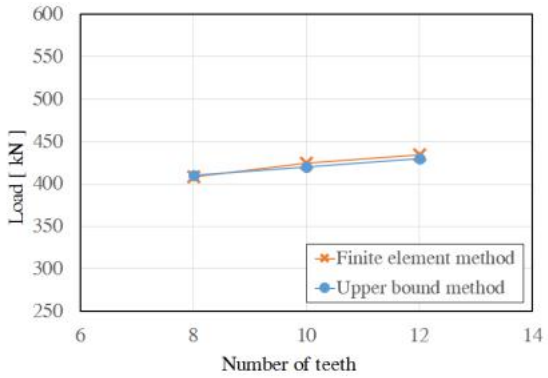

(a) load and number of teeth

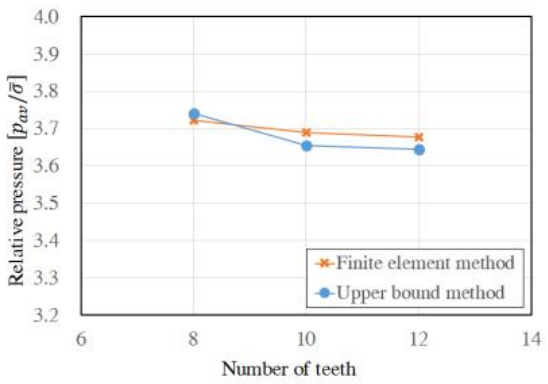

(b) relative pressure and number of teeth

Fig. 6 Comparisons of upper bound analysis and FEM at nominal diameter 0.71 of internal spline

Fig. 5 and Fig. 6 show comparison between upper bound result and FEM one and the two results of forming load and relative pressure are coincide each other. Fig. 5 shows forming load and relative pressure varying according to nominal diameter ratio under the condition of same number of teeth and tooth height. It is shown that the form-ing load is increased by the increasing of nominal diameter ratio. However, in case of relative pressure, it is decreased until 0.7 of nominal diameter ratio and then increased. The higher nominal diameter ratio has the bigger punch area while the extruded material area is decreased and this makes the relative pressure higher. Because both the form-ing load and the relative pressure get increase again from 0.7 of nominal diameter ratio, punch fracture should be taken into account in design. Fig. 6 shows varying forming load and relative pressure according to number of teeth under the nominal diameter ratio and tooth height keep same. Every two number of teeth leads about 10kN in-crease of forming load. The relative pressure acting on punch surface caused by numerical increase of teeth de-creased because rate of forming load growth is smaller than that of punch area. And the main factor impacting on forming load determination is nominal diameter ratio rather than number of teeth. Therefore, it is reasonable to select machine capacity with only nominal diameter ratio in backward extrusion for internal spline.

4. Experiment of Backward Extrusion

Backward extrusion experiments have been down with 75º of punch tip conical angle of, 12 teeth, 0.71 of nominal diameter ratio. The material is SCM 435 of 20 mm in diameter and 20 mm in height.

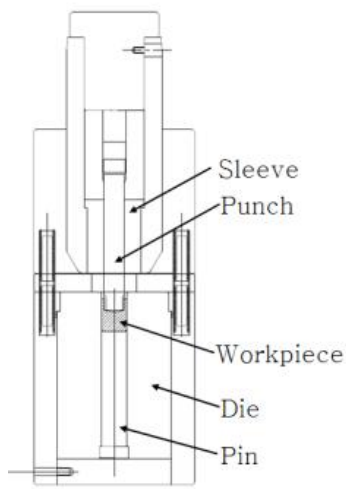

Fig. 7 Schematic drawing of backward extrusion dies for internal spline

The test was done in hydraulic pressure with tools shown in Fig. 7. To measure forming load during forming process, strain gauges have been implemented on tool surfaces and amplitude with QuamtrmX MX1615B by HBM. Fig. 8 shows extruded internal spline. No flaws such as folding or under filling were detected and the reclined tooth shape at the entrance of hole which is same to Fig. 3 result was seen. Fig. 9 shows forming load from backward extrusion experiment compare to upper bound FEM simulation results. The maximum forming load of experiment, upper bound and FEM are about 410kN, 434kN and 435kN, respectively.

The maximum forming load of upper bound method is 5.8% higher than that of experimental one. Upper bound method predicts at least same or even higher forming load compare to exact load to plastic flow of material. Regarding this characteristic of upper bound method, it is concluded that the predicted load by upper bound method is well coincide with experiment and FEM results as well. The velocity field suggested in this paper is reasonable and useful to predict forming load, and the internal spline machining could be replace by backward extrusion.

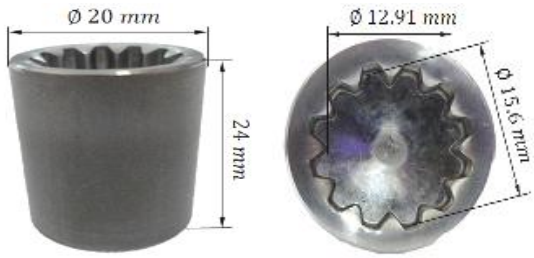

Fig. 8 Experimental results of internal spline

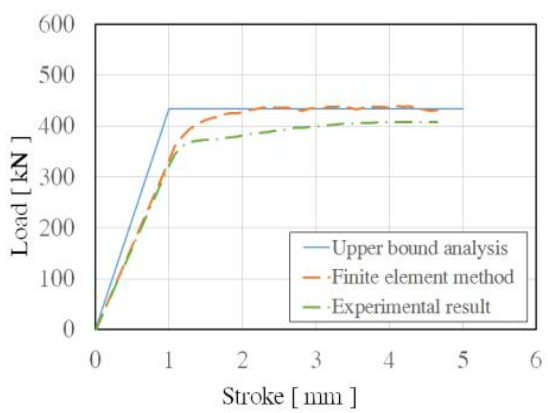

Fig. 9 Comparisons of forming loads between upper bound analysis, FEM and experimental result

5. Conclusions

Backward extrusion of internal spline has been analyzed with upper bound method and rigid plastic analytical software of DEFORM-3D. A kinematically admissible velocity field has been suggested and upper bound solution was calculated. Experimental set up for internal spline has been established for 0.71 of nominal diameter ratio and done experiments with 20 mm in diameter and 20 mm in height solid billet. From these, it is concluded that;

1. The machine capacity could be decided by nominal diameter ratio because nominal diameter ratio is main factor affecting on forming load compare to number of teeth.
2. The suggested velocity field is useful to predict forming load of internal spline backward extrusion and its maximum load is 5.8% higher than that of experiment.
3. No forging flaw like folding or under filling was detected and this means that the backward extrusion process could replace the machining in internal spline manufacturing.

This research was supported by project of Industrial core technology development “Develop ment of Metal/CFRP Hybrid Riveting Technology with 1 million cycle Fatigue Durability and 80 MPa Joining Strength, No.10083614”

References

1. Cho, C. Y., Park, S. W., Lee, J. O., Seo, H. S. and Lee, J. M., “Development of Backward Extrusion Process for Large-size Tube”, Proceedings of The Korean Society for Technology of Plastics Academic Conference, pp. 462~465. 2010.
2. Chen, Q., Xia, X., Yuan, B., Shu, D. and Zhao, Z., “Microstructure Evolution and Mechanical Properties of 7A09 High Strength Aluminium Alloy Processed by Backward Extrusion at Room Temperature”, Materials Science and Engineering: A, Vol. 588, pp. 395~402. 2013.
3. Yang, D. Y., Bae, W. B. and Lee, D. H., “Backward Extrusion of Internally Elliptic-Shaped Tubes from Round Billets”, Korea Society for Precision Engineering, No. 6, pp. 46~58. 1991.
4. Lee, H. I., Kim, J. K., Hwang, B. C. and Bae, W. B., “A UBET Analysis on the combined extrusion of a wrench bolt”, Proceedings of the Korean Society for Precision Engineering Academic Conference, pp. 1044~1047. 1999.
5. Wang, C. B., Kim, D. J., Lim, S. J., Kim, Y. K. and Kim, M. E., “Analysis for Cold Extrusion Process of Internal Spline Using the Tube”, The Korea Society for Technology of Plasticity, No. 5, pp. 403~406. 2006.
6. Wang, C. B., Lim, S. J. and Park, Y. B., “Effect of the Design Parameter for Internal Spline Forming Using the Tube”, the Korean Society for Technology of Plastics, Vol. 15, No. 88, pp. 512~517. 2006.